GS-3 Mineral chemistry of chromite in the Mayville intrusion: evidence for petrogenesis and linkage to the Bird River sill in the Neoarchean Bird River greenstone belt, southeastern Manitoba (parts of NTS 52L5, 6, 12)

by X.M. Yang and H.P. Gilbert

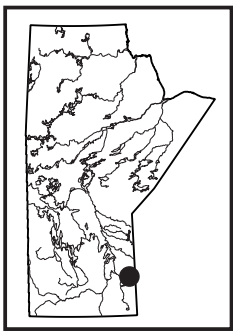

Yang, X.M. and Gilbert, H.P. 2014: Mineral chemistry of chromite in the Mayville intrusion: evidence for petrogenesis and linkage to the Bird River sill in the Neoarchean Bird River greenstone belt, southeastern Manitoba (NTS 52L5, 6, 12); *in* Report of Activities 2014, Manitoba Mineral Resources, Manitoba Geological Survey, p. 32–48.

Summary

In 2014, the Manitoba Geological Survey completed bedrock mapping in the northern arm of the Bird River greenstone belt of the western Superior province, southeastern Manitoba. The project aim was to provide fundamental geoscientific information to assist mineral exploration, in particular for magmatic Ni–Cu–platinum group element (PGE)–Cr mineralization associated with mafic–ultramafic intrusions in the region. Because mafic–ultramafic rocks are readily altered by deformation, metamorphism, magmatism and related hydrothermal systems, their primary mineral assemblages and geochemical composition are typically modified, requiring more robust geochemical techniques to 'see through' these effects. Consequently, the mineral chemistry of chromite, which is highly refractory and resistant to chemical modification, has been examined to help evaluate the affinity and fertility of mafic–ultramafic systems in the Bird River belt.

This report presents chemical composition data on chromite from the Neoarchean Mayville mafic–ultramafic intrusion (MI) in the north arm of the Bird River greenstone belt, and compares them to that of chromite in the Bird River sill (BRS) in the southern limb of the belt, in order to provide insight into the magmatic affinity, magmatic processes, tectonic setting and petrogenetic relationships. Chromite in the MI is characterized by higher Fe-number (Fe# = 100 x Fe^{2+} / [Fe^{2+} + Mg^{2+}]) and Al/Mg ratio, variable Cr-number (Cr# = 100 x Cr^{3+} / [Cr^{3+} + Al^{3+}]) and lower Mg-number (Mg# = 100 x Mg^{2+} / [Mg^{2+} + Fe^{2+}]) compared to that in the BRS. This indicates that the parent magma(s) to the MI is/are of tholeiitic affinity, like those of the BRS but more evolved, and may have been derived from subcontinental aluminous lithospheric mantle enriched by slab melt(s) related to plate subduction. In contrast, the parental magma(s) to the BRS was/were less evolved and may have been sourced from more depleted subcontinental lithosphere mantle. Although the MI is synchronous with the BRS and both are thus related to the extensive 'Bird River magmatic event' proposed by Houlé et al. (2013), they are interpreted to result from different petrogenetic processes that reflect either different sources or degrees of differentiation. This study complements detailed bedrock mapping and lithogeochemical investigations, and indicates that the MI is fertile for Ni-Cu-PGE mineralization, in accord with the widespread occurrence of contact-style magmatic sulphide mineralization near the base of the heterolithic breccia zone (HBZ) and at the basal contact of the intrusion. Furthermore, the MI is prospective for reef-style, stratiform PGE mineralization in transitional and/or contact zones between major rock units, and for stratiform chromitite mineralization as demonstrated by the presence of massive chromitite bands and disrupted chromitite-pyroxenite layers within the HBZ.

Introduction

In 2014, the Manitoba Geological Survey (MGS) continued the multiyear mapping project in the northern arm of the Bird River greenstone belt (BRGB) of the western Superior province in southeastern Manitoba (Figure GS-3-1). This project has been conducted by the MGS in collaboration with the Geological Survey of Canada (GSC) through a Targeted Geoscience Initiative 4 program, which was supported by Mustang Minerals Corp. (MMC). The main objectives of the project are to

- update the regional bedrock map in the Cat Creek and Cat Lake–Euclid Lake areas;
- address the geological evolution and geodynamic environment of the BRGB; and
- assess the metallogeny of magmatic Ni-Cu-PGE sulphide and Cr mineralization associated with mafic–ultramafic intrusions within the BRGB.

The northern arm of the BRGB, including the Mayville mafic–ultramafic intrusion (MI) and surrounding rocks in the Cat Creek area, were mapped by the MGS in 2012 at 1:12 500 scale. This bedrock geology map has been revised, expanded and upgraded to 1:10 000 scale (Yang, 2014) based on data acquired in the last two years (Figure GS-3-2). The MI is a composite layered intrusion, comprising dominantly gabbroic–anorthositic rocks with minor ultramafic components, which was intruded into mid-ocean-ridge basalt (MORB)–type basalts overlying Mesoarchean basement represented by the Maskwa Lake batholith I (Yang et al., 2012, 2013). Bedrock mapping and exploration drilling indicate that Ni-Cu-PGE-Cr mineralization is hosted mostly in the mafic–ultramafic units in the lower part, and/or at the base, of the MI. Since the MI underwent regional metamorphism and was intruded

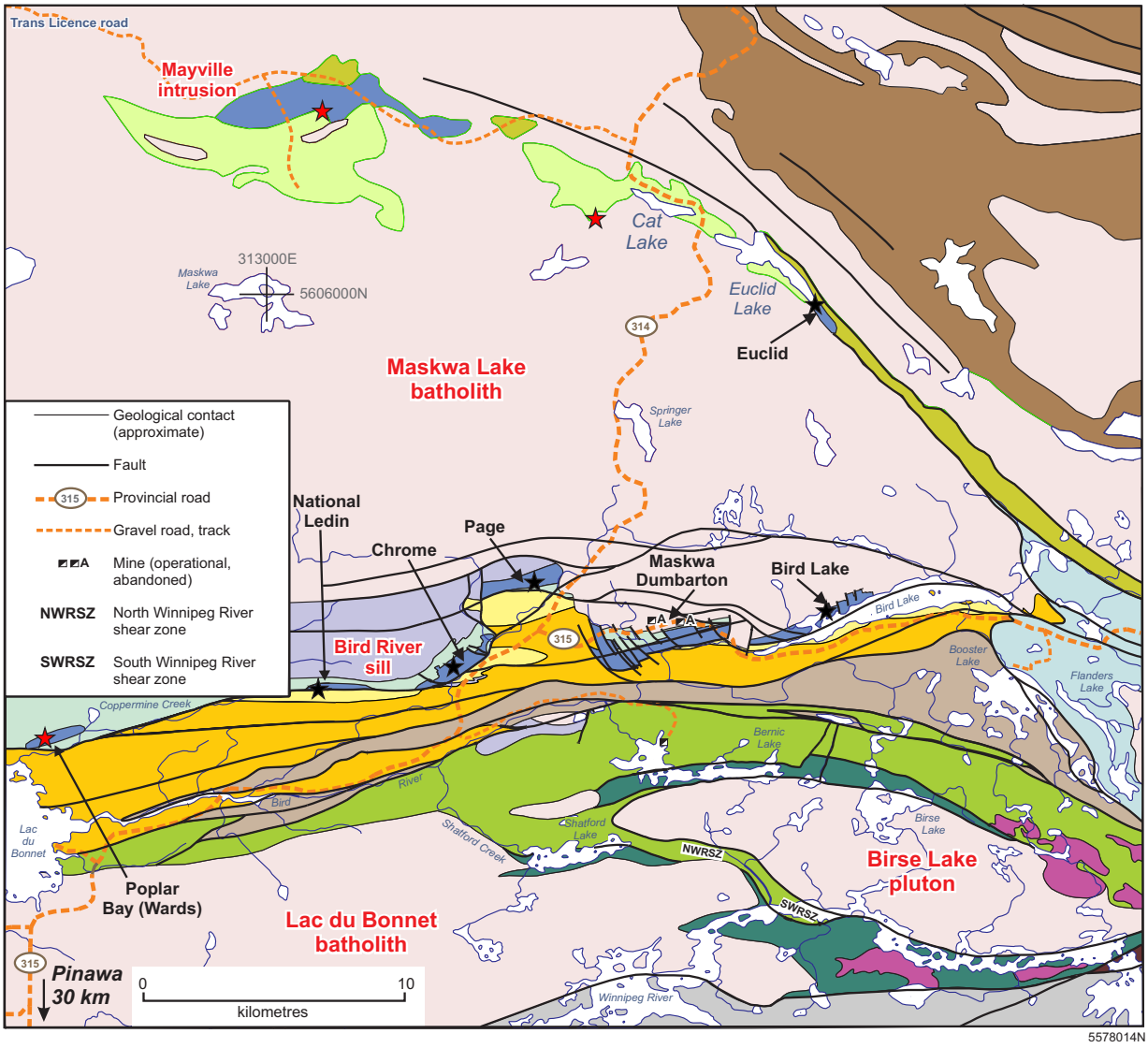

Bird River subprovince

INTRUSIVE ROCKS

- Pegmatitic granite
- Granite, granodiorite, tonalite
- Gabbro, diorite, quartz diorite
- Pyroxenite, anorthosite, gabbro

LATE SEDIMENTARY ROCKS

Flanders Lake formation

- Arenite, polymictic conglomerate

Booster Lake formation

- Greywacke, siltstone

VOLCANIC AND SEDIMENTARY ROCKS

BIRD RIVER BELT SOUTH PANEL

Bernic Lake formation

- Heterolithic volcanic breccia, rhyolite, basalt, andesite

Eaglenest Lake formation

- Greywacke, siltstone

Southern MORB-type formation

- Basalt, aphyric; gabbro

BIRD RIVER BELT NORTH PANEL

Diverse arc assemblage

- Massive to fragmental, mafic to felsic volcanic and sedimentary rocks

Peterson Creek formation

- Massive to fragmental felsic volcanic rocks

Northern MORB-type formation

- Basalt, aphyric; gabbro

CAT LAKE AREA

- Sedimentary and volcanic rocks, related gneiss
- Tholeiitic basalt

English River subprovince

- Paragneiss, granitoid intrusive rocks, migmatite, pegmatite

Winnipeg River subprovince

- Tonalite, granodiorite, granitoid gneiss

- Ni-Cu-PGE deposit/occurrence
- Cr-PGE deposit/occurrence

Figure GS-3-1: *Regional geology between Cat Lake–Euclid Lake and the Winnipeg River, southeastern Manitoba, showing the southern arm of the Bird River greenstone belt between Lac du Bonnet and Flanders Lake, and the northern arm extending as far as the Mayville intrusion. Locations of chromite deposits (e.g., Chrome property, Euclid Lake) marked by black stars.*

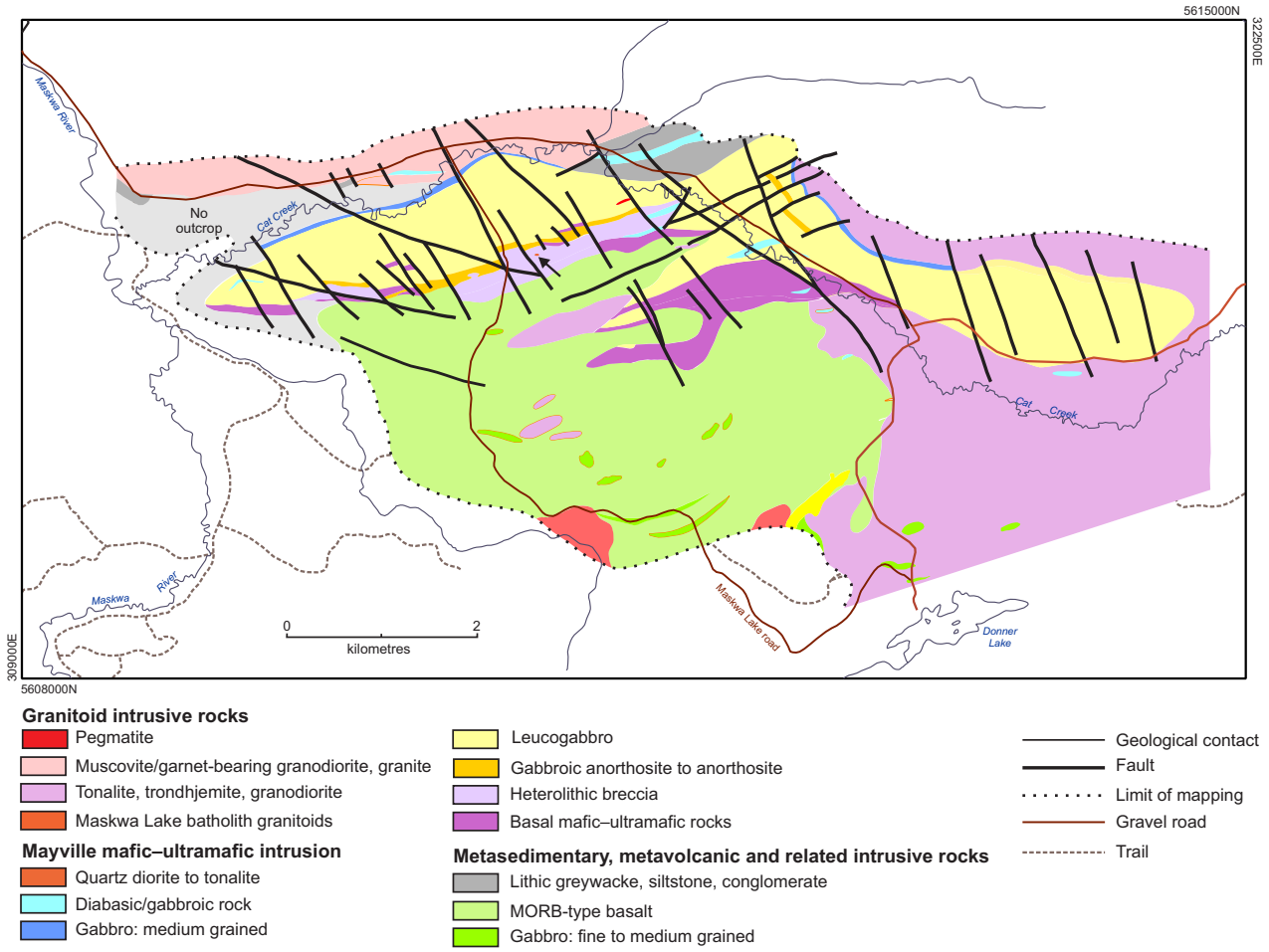

***Figure GS-3-2**: Simplified geological map of the Neoarchean Mayville intrusion in the northern arm of the Bird River greenstone belt, southeastern Manitoba (modified after Yang, 2014). A quartz diorite to tonalite (unit 10) dike (or dikes) within the Mayville intrusion is/are indicated by the orange dot (not to scale) at the end of the black arrow.*

by Neoarchean tonalite, trondhjemite and granodiorite (TTG; e.g., Peck et al., 2002; Yang and Gilbert, 2014), its primary mineral assemblages and lithogeochemical characteristics were strongly modified, although magmatic textures are generally well preserved (Peck et al., 1999; Yang et al., 2011, 2012). Due to its highly refractory nature, chromite in the MI provides a record of the primary geochemical signatures of the magmas, which are essential in evaluating its fertility for Ni-Cu-PGE-Cr mineralization and for exploration targeting.

This report concentrates on the Neoarchean MI (2742.8 ±0.8 Ma; see Houlé et al., 2013) by using chromite chemistry as a tool to investigate its magmatic affinity, magmatic processes and tectonic setting(s), and to compare them with those of the Bird River sill (BRS) in the southern limb of the BRGB in order to investigate the possibility of a petrogenetic relationship.

A brief background on chromite studies is provided before the results of work on the Mayville chromite are presented, to show the important role played by this mineral in investigations of petrogenesis of mafic–ultramafic rocks and in mineral exploration.

Brief review of chromite studies

Chromite ($Fe^{2+}Cr_2O_4$) is an end member of the spinel group of minerals, whose formula is AB_2O_4 (where A is Fe^{2+}, Ni^{2+}, Mn^{2+}, Co^{2+} or Zn^{2+} in four-fold co-ordination *T* sites and B is Cr^{3+}, Fe^{3+}, Al^{3+} or Ti^{4+} in six-fold co-ordination *M* sites; Deer et al., 1962, 1992). Spinel group minerals have long been used as 'petrogenetic indicators' (Irvine, 1965, 1967), because 1) they crystallize over a wide range of conditions from mafic–ultramafic magmas; 2) are among the first phase(s) to crystallize; 3) display a wide range of solid solution; and 4) are relatively refractory and resistant to alteration and metamorphism compared to other high-temperature magmatic silicate minerals, such as olivine or orthopyroxene (Peck and Keays,1990; Barnes, 1998, 2000; Barnes and Roeder,

2001; Sobolev and Logvinova, 2005; Rollinson et al., 2010; Krause et al., 2011; Voigt and von der Handt, 2011).

The cores of chromite crystals may retain their original magmatic chemistry at metamorphic temperatures of up to 500°C (Barnes, 1998) or even higher (Rollinson et al., 2010). Therefore, chromite chemistry has proven to be an effective tool to investigate magma types, magmatic processes and tectonic settings in metamorphosed mafic–ultramafic intrusions (Irvine, 1965; Roeder, 1994; Stowe, 1994; Barnes, 1998, 2000; Barnes and Roeder, 2001; Kamenetsky et al., 2001; Arif and Jan, 2006). Chemical composition of spinel minerals can also be used to identify Ni-mineralized and -barren mafic–ultramafic intrusions (Yang et al., 1994; Barnes and Tang, 1999; Barnes and Kunilov, 2000). Therefore, spinel is one of the best index minerals for Ni-Cu-PGE-Cr exploration. Moreover, chromite included in diamonds displays a relatively narrow Cr# range ($100 \times Cr^{3+}/[Cr^{3+} + Al^{3+}] = 75–90$) but variable Mg# ($100 \times Mg^{2+}/[Mg^{2+} + Fe^{2+}] = 50–80$), thus making it an ideal indicator for diamond exploration (Sobolev and Logvinova, 2005).

Previous work

Chromite and chromitite seams occur in various mafic–ultramafic intrusions, including the MI and BRS in the northern and southern arms of the BRGB, respectively (Figure GS-3-1; Stevenson et al., 2001; Bailes et al., 2003; Lemkow et al., 2006; Gilbert et al., 2008). Multiple generations of deformation, metamorphism and magmatism have influenced the entire belt (Trueman, 1980; Duguet et al., 2009).

Mayville intrusion

The MI is a layered composite intrusion consisting predominantly of gabbroic–anorthositic rocks with minor ultramafic components (Figure GS-3-2; Yang, 2014). Chromite is present mostly in the heterolithic breccia zone (HBZ; Peck et al., 1999; Yang et al., 2012) as 1) chromitite bands or layers; 2) disseminations in pyroxenite and gabbro; and 3) discrete crystals in the reaction zones between leucogabbro (blocks) and ultramafic rocks in the MI, as described by Hiebert (2003). Chromitite layers up to 0.4 m thick, consisting of ~30–50 mode % chromite, plus amphibole, chlorite and minor sulphide, occur within the upper HBZ (Figure GS-3-3a, b). Some chromite grains contain exsolution lamellae of ilmenite and/or rutile (Figure GS-3-3c), confirming the observations of Hiebert (2003). This style of chromitite is similar to the BRS, where the Chromitiferous zone, comprising chromitite bands or layers, is also present at the top of the Ultramafic series (Scoates et al., 1986, 1989; Williamson, 1990). Some chromitite layers in pyroxenite are strongly magnetic, whereas others are lens-like rafts that are not magnetic (Figure GS-3-3d, e). Disseminated chromite usually occurs in ultramafic dikes in the heterolithic unit, which contains scattered disseminated pyrrhotite and chalcopyrite (Figure GS-3-3f). It is noted that some chromite crystals contain rounded inclusions of silicate melt (Figure GS-3-3g), suggesting that chromite crystallized from a silicate melt. Compositional zoning is not uncommon in Mayville chromite (Figure GS-3-3h), indicating that it was likely buffered by the melt composition. Pyrrhotite inclusions are evident in chromite, suggesting that sulphide saturation may have occurred earlier (Hiebert, 2003; Yang et al., 2011, 2012), perhaps resulting in Ni, Cu and PGE depletion in the evolved residual magma(s).

Hiebert (2003) investigated the chemical composition of chromite from the MI, concluding that it is generally characterized by much lower MgO/(MgO+FeO) ratios than those in the BRS (as determined by Gait, 1964). This suggests that the magmas from which the MI crystallized may have been relatively more evolved, consistent with petrological and lithogeochemical features (Theyer, 1991, 2003; Peck et al., 1999, 2000; Yang et al., 2011, 2012). It is noted that Hiebert (2003) only analyzed five elements (i.e., Al_2O_3, MgO, Cr_2O_3, TiO_2, FeO). Full characterization of the chemistry of chromite, however, also requires analysis of NiO, CoO, MnO and ZnO (see Barnes and Roeder, 2001; Rollinson et al., 2010).

In this study, 17 samples from the MI were collected for petrographic investigation and chemical analysis of chromite to characterize the chemical signatures and magmatic affinity, and compare them with those of chromite in the Bird River sill. The nature of the parent magma from which the MI formed is also assessed using chromite chemistry. As mentioned in the above brief review of chromite studies, the cores of refractory chromite grains may record information regarding the magma from which it crystallized, whereas rim composition of the chromite may reflect re-equilibrium with interstitial residual melt (silicate liquid).

Bird River sill

In the BRS, six groups of chromitite layers occur in the Chromitiferous zone, which is about 60 m thick and consists of alternating layers of peridotite and chromitite (Figure GS-3-4; Scoates et al., 1986, 1989; Williamson, 1990). The chromitite layers or bands are well exposed at the Chrome property (Figure GS-3-1), where the entire stratigraphy of the BRS is also exposed. Three representative samples were collected from the Upper Main section of the Chromitiferous zone for chemical analysis of chromite in this study, and previous chromite data from Gait (1964) were also compiled to characterize the chemical composition of chromite in the BRS. Type chromitite from the BRS is shown in Figure GS-3-5.

The chemistry of chromite in the BRS was studied by Bateman (1945) after this mineral had been identified (Brownell, 1942; Bateman, 1943), suggesting an excess of Fe_2O_3 present as exsolved hematite in some chromite

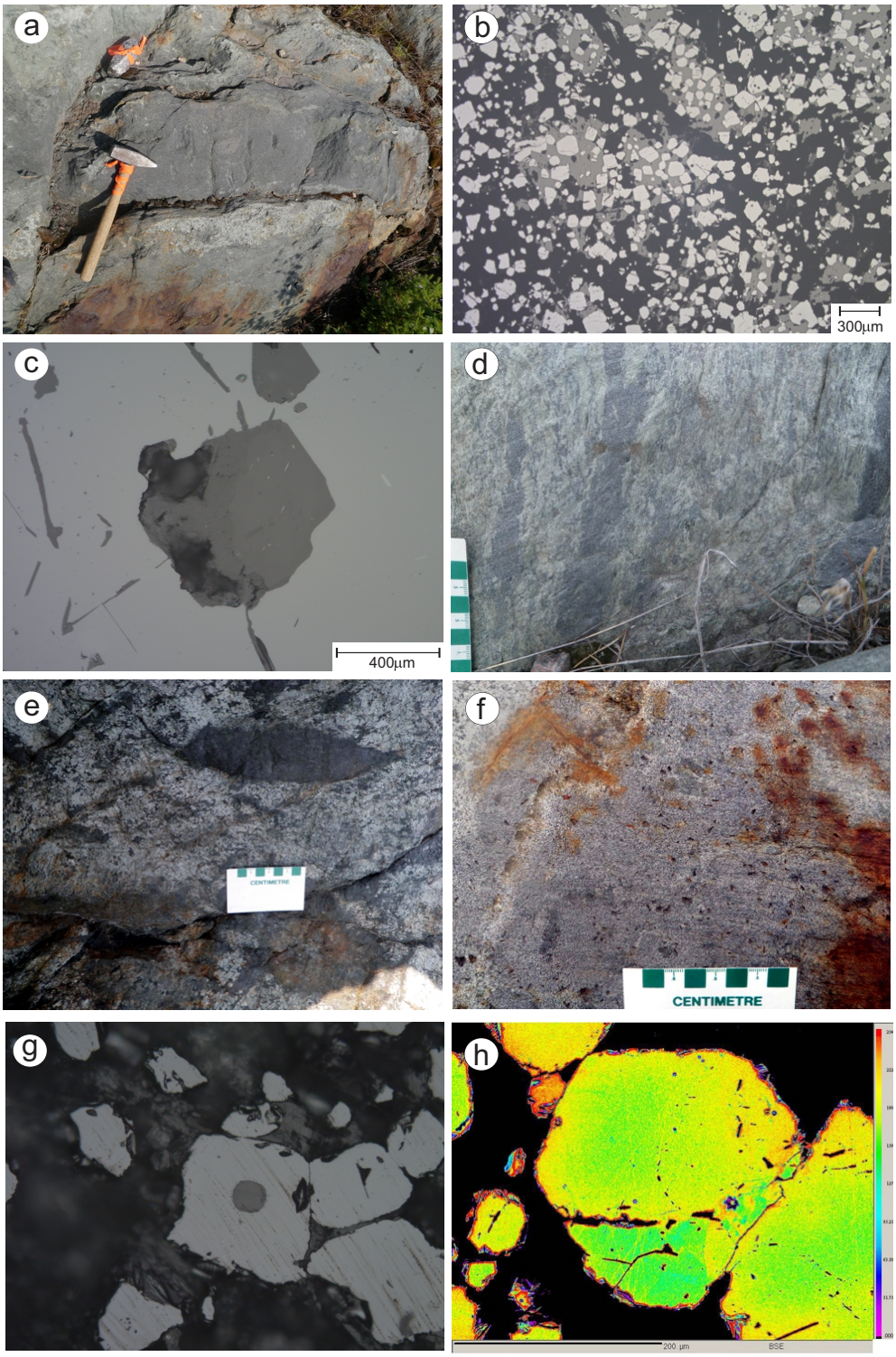

***Figure GS-3-3**: Field photographs of chromite occurrences and representative photomicrographs of chromite crystals in the Mayville intrusion, Cat Creek area, southeastern Manitoba: **a)** disrupted, ~40 cm thick, nonmagnetic chromitite band in pyroxenite (UTM Zone 15N, 314616E, 5612596N, NAD83) from the heterolithic breccia unit; **b)** euhedral to subhedral chromite crystals (scale bar is 100 µm) in the massive chromitite band (sample 111-12-500B1; location same as (a); reflected polarized light [RPL]); **c)** exsolved lamellae in a chromite crystal (sample111-12-500B1; RPL); **d)** strongly magnetic chromitite layers in pyroxenite (UTM 314606E, 5612599N); **e)** lens-like chromitite raft in pyroxenite (UTM 314606E, 5612599N); **f)** disseminated chromite in an ultramafic dike from the heterolithic unit that also contains scattered disseminated pyrrhotite and chalcopyrite (UTM 314616E, 5612473N); **g)** spherical inclusion of silicate melt, about 25 µm in size, in a subhedral chromite crystal with resorbed edges (sample 111-12-500B1; RPL); **h)** back-scattered electron image with pseudocolour, showing compositional zonation or heterogeneities in chromite (sample 111-12-500B1).*

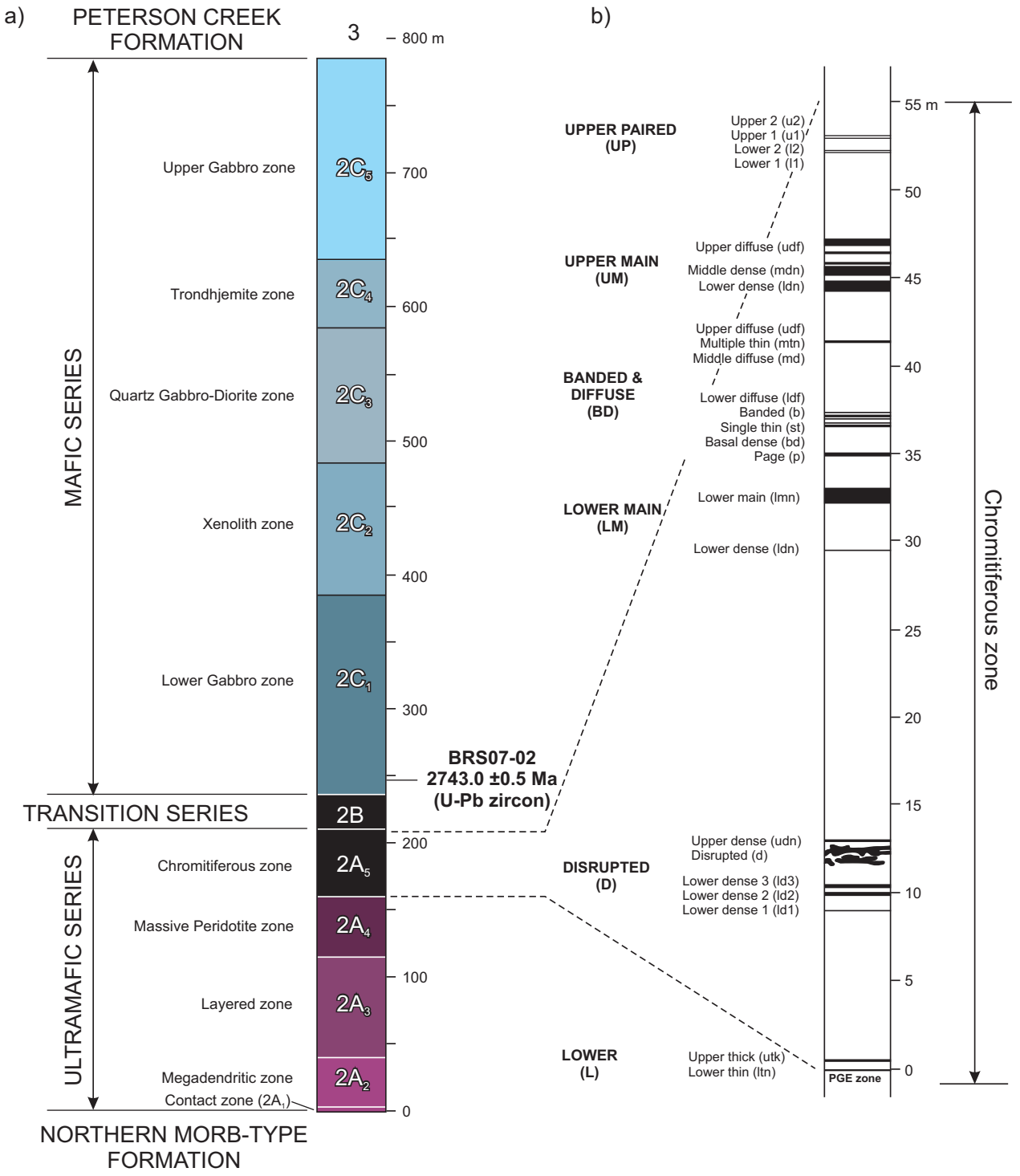

Figure GS-3-4: *Stratigraphic column of the Bird River sill* ***(a)*** *and subdivision of its Chromitiferous zone into six groups* ***(b)*** *at the Chrome property in the southern arm of Bird River greenstone belt, southeastern Manitoba: Lower, Disrupted, Lower Main, Banded and Diffuse, Upper Main and Upper Paired sections (after Williamson, 1990). Also shown is the approximate stratigraphic position of the U-Pb age determination (2743.0 ±0.5 Ma) by Scoates and Scoates (2013), who interpreted it as the crystallization age of the Bird River sill.*

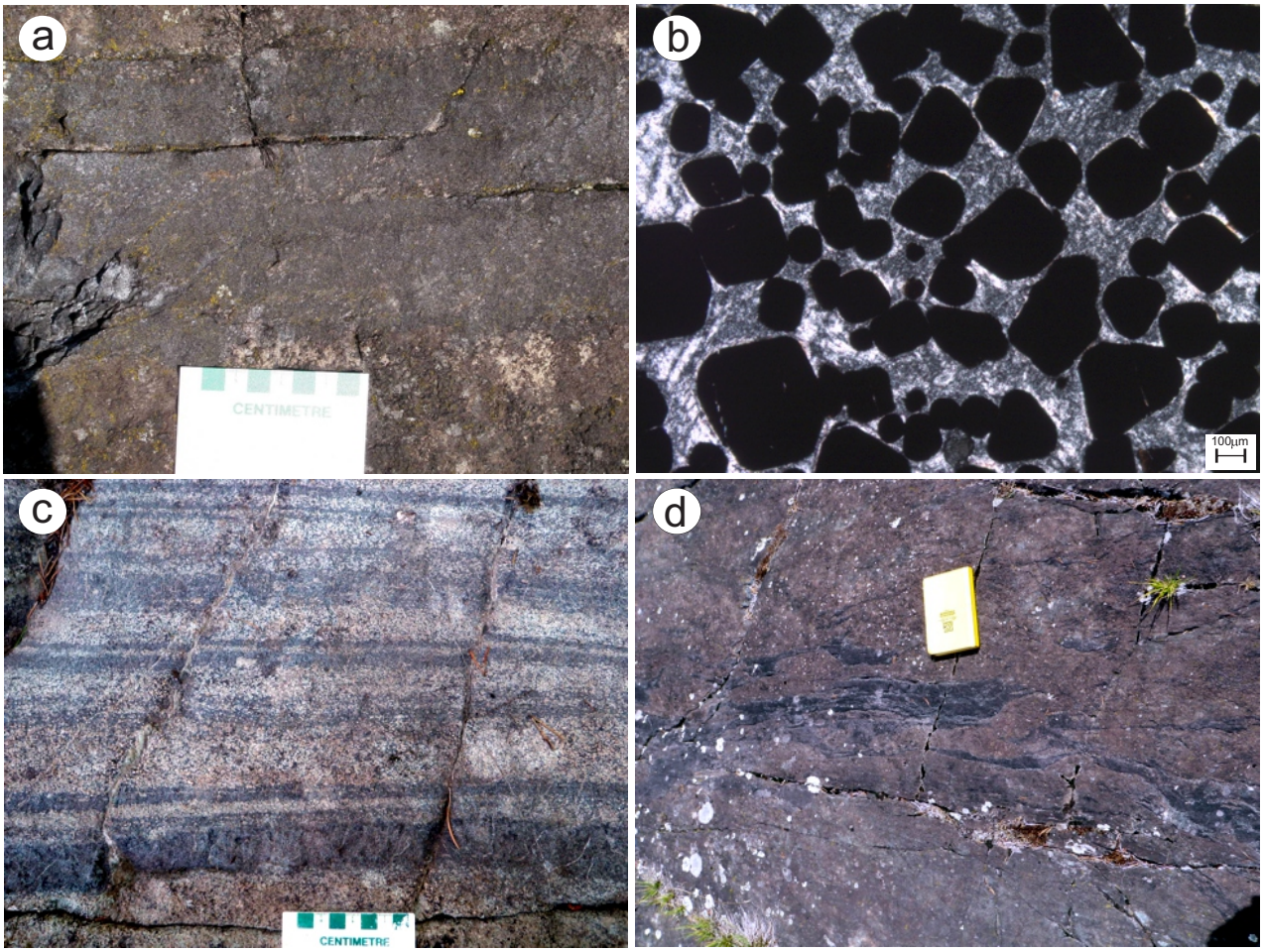

Figure GS-3-5: *Field photographs of chromite occurrences and representative photomicrograph of chromite crystals from the Chrome property, Bird River sill, southeastern Manitoba:* ***a)*** *massive, ~20 cm thick, nonmagnetic chromitite band in peridotite (UTM Zone 15N, 318414E, 5592677N, NAD83);* ***b)*** *euhedral to subhedral chromite crystals (scale bar is 100 µm) in the massive chromitite band (sample 111-11-18; location is the same as (a); transmitted plane-polarized light;* ***c)*** *multiple thin chromitite layers in peridotite (UTM 318425E, 5592685N);* ***d)*** *disrupted chromitite subunit hosted by peridotite (UTM 318270E, 5592688N).*

specimens. This finding was confirmed by Gait (1964) through a heating experiment in which a hematite rim and/or laminae exsolved from chromite on heating at 1000°C in a furnace without controlling oxygen fugacity.

Scoates et al. (1986, 1989) presented a plot of Cr# versus Mg# to portray the chemical compositions of chromite from the six chromitite layer groups in the BRS, and suggested that an earlier magmatic trend controlled by fractionation of the ultramafic–mafic magmas led to increasing Cr# (from ~50 to 70) with decreasing Mg# (from 62 to 15). These authors also suggested that a late metamorphism may have elevated the Cr# (from 70 to 100) within a narrow range of Mg# (20 to 5). They attributed the magmatic trend to reaction of cumulus chromite with intercumulus liquid (silicate melt) or silicate minerals during subsolidus cooling, and the metamorphic trend to the growth of ferrichromite as rims around cores of magmatic chromite during regional metamorphism. Scoates et al. (1989) pointed out that the ratio of chromite to silicate is a key factor controlling the interaction between chromite and silicate during metamorphism. For example, chromite from chromite-silicate cumulate with a ratio of about 1:1 was little affected by metamorphism and retains the signature of a magmatic trend, whereas chromite in olivine-chromite cumulate shows significant Fe enrichment because of the lower chromite-silicate ratio, resulting in a metamorphic trend.

Ohnenstetter et al. (1986) determined the chemical composition of chromite in the Upper Main chromitite layers defined by Scoates (1983), finding trends similar to those identified by Scoates et al. (1986, 1989). Generally, chemical composition of chromite from the BRS is consistent with those of stratiform chromite deposits associated with mafic–ultramafic intrusions, as summarized in Duke (1983).

A major PGE concentration zone (reef), ~1 m thick, is present at the base of the Chromitiferous zone (Figure

GS-3-4), which occurs at the top of the Ultramafic series. This PGE zone is associated with Lower group chromitite (Figure GS-3-4) and with a subjacent interval of peridotite containing sparse, irregularly disseminated sulphide minerals (Scoates et al., 1989; Peck et al., 2002). It extends laterally about 800 m along the zone, and seems to be stratiform.

Tiny laurite (RuS_2) inclusions, 1.5–12 μm in size, together with rutheniridosmine (Os, Ir, Ru alloy), in chromite from the Chromitiferous zone are associated with pyrrhotite, chalcopyrite and pyrite (Talkington et al., 1983; Ohnenstetter et al., 1986). This suggests earlier sulphide saturation in the BRS. Ruthenium (and Ir, Os) appears to have higher capacity to combine with S^{2-} than either Ni or Fe in ultramafic melt because sulphide inclusions are dominated by laurite.

Present study

Petrography

Massive fine-grained chromitite consists of 35–50 modal % euhedral to anhedral chromite, 0.02–0.3 mm in diameter, embedded in a groundmass of serpentine and chlorite (Figure GS-3-3b, -5b). Most chromite grains are unaltered, but some display minor chloritic alteration. Some chromite crystals contain rounded silicate inclusions and others have sulphide inclusions, indicating that chromite crystallized from sulphide-saturated silicate magma(s). Compositional zonation is common, mostly with an FeO^t-enriched rim and Cr_2O_3-rich core (Figure GS-3-3h). However, reverse zoning is also evident. Opaque minerals are dominantly chromite, and minor ilmenite and rutile.

Disseminated chromite also occurs in pyroxenite and gabbroic rocks from the MI. The ultramafic rock is commonly coarse grained, showing adcumulus texture, and consists dominantly of hornblende (as a result of alteration of pyroxene, mostly clinopyroxene). Hornblende crystals are euhedral to subhedral, and constitute more than 90% of the mode. Some hornblende grains are strongly altered to chlorite and carbonate, and magnetite. Recrystallization of some grains is manifested by smaller amphibole aggregates. Disseminated chromite occurs as inclusions in hornblende grains, and pyrite and pyrrhotite are interstitial.

Mineral chemistry

Analytical method

The chemical composition of chromite was analyzed by electron probe microanalyzer (EPMA). The analytical work was conducted in wavelength-dispersion mode on a Cameca SX-100 electron microprobe at the University of Manitoba. Operating conditions were 15 kV accelerating voltage, 20 nA beam current and a 20-second counting interval for both peak and total background. The beam size was set at 10 μm, except for very small chromite grains that were analyzed by using a focused beam (<1 μm). A combination of various minerals and metal standards were used to analyze for SiO_2 (0.06), TiO_2 (0.04), V_2O_5 (0.05), Al_2O_3 (0.02), Cr_2O_3 (0.05), FeO (0.06), MnO (0.03), MgO (0.03), CoO (0.06), NiO (0.07) and ZnO (0.10); the number in brackets after each oxide indicates analytical uncertainty in percent for that element. Raw data were calibrated with PAP matrix corrections. In each sample, several chromite grains were analyzed based on textural relation and analyzed positions in a crystal (e.g., rim, middle, core). An average of these analytical results was taken to represent the typical composition of the chromite in each sample, together with standard deviation. Formula calculations of chromite are based on four atoms of oxygen, and their ferric/ferrous ratios are calculated by stoichiometry and charge balance using the method of Barnes and Roeder (2001). Table GS-3-1 presents the chemical composition and structural formulas of chromite in representative samples collected from the MI and the BRS.

Chromite chemistry

Nomenclature of spinel group minerals used in this study strictly follows the recommendations of International Mineralogical Association (Nickel, 1992). Spinel minerals are named based on the most abundant trivalent cations: chromite (dominated by Cr^{3+}), spinel (Al^{3+}) or magnetite (Fe^{3+}). Accordingly, spinel minerals in the MI and the BRS are chromite that is dominated by Cr^{3+} (Table GS-3-1). Chromite in the MI has a maximum Cr/Fe^t ratio of 1.1, whereas those in the BRS vary up to 1.8. These ratios are well within the range of stratiform chromite deposits associated with layered mafic–ultramafic intrusions but much lower than those of podiform chromite deposits related to ophiolite suites (Stowe, 1994).

It is worth noting that chromite in the BRS displays a range of Mg# from 19 to 50, but maintains a narrow, relatively high range of Cr# (52 to 76). In contrast, chromite in the MI has a range of Cr# from 31 to 83, with only a small variation in Mg# (10 to 23; see below).

Chemical composition of chromite in the MI and the BRS is well portrayed in a set of compositional diagrams suggested by Barnes and Roeder (2001), based on two common projections of the spinel prism of Stevens (1944). The Cr^{3+}-Al^{3+}-Fe^{3+} ternary diagram (Figure GS-3-6) represents the projection onto the end face of the prism; diagrams (not shown) of $Cr^{3+}/(Cr^{3+}+Al^{3+})$ and $Fe^{3+}/(Fe^{3+}+Cr^{3+}+Al^{3+})$ versus $Fe^{2+}/(Mg^{2+}+Fe^{2+})$ (i.e., Fe#) represent their mutual relations to Fe#. Plots (not shown) of TiO_2 against $Fe^{3+}/(Fe^{3+}+Cr^{3+}+Al^{3+})$ and against Fe# are also used to explore their compositional variations.

On the Cr^{3+}-Al^{3+}-Fe^{3+} ternary diagram, two populations of chromite are evident (Figure GS-3-6). One group displays an Fe-Ti trend and exhibits characteristics

Table GS-3-1: Chemical composition (wt. %) and structural formulas of chromite in representative samples from the Mayville intrusion and Bird River sill, Neoarchean Bird River greenstone belt, southeastern Manitoba.

Sample:	111-12-500B1		111-11-12	111-11-20		111-11-18		111-11-21	
Intrusion:	MI		MI	BRS		BRS		BRS	
Rock type:	Chromitite		Pyroxenite	Chromitite		Chromitite		Chromitite	
Mineral:	Chromite		Chromite	Chromite		Chromite		Chromite	
No. of grains:	4		1	8		4		4	
No. of analyses:	13		1	14		5		7	
	Av.	**SD**	**Core**	**Av.**	**SD**	**Av.**	**SD**	**Av.**	**SD**
SiO_2	0.01	0.01	0.16	0.02	0.01	0.03	0.02	0.07	0.11
TiO_2	1.17	0.06	0.50	0.44	0.20	0.36	0.04	1.26	0.04
V_2O_5	0.36	0.04	0.25	0.29	0.03	0.21	0.03	0.36	0.02
Al_2O_3	12.78	0.51	17.49	16.06	2.39	17.84	0.38	14.45	0.43
Cr_2O_3	37.22	0.29	30.81	44.37	3.62	41.57	0.25	43.02	0.90
FeO^t	44.41	0.39	43.98	28.32	2.18	30.09	1.30	30.61	3.64
FeO	32.26	0.14	31.95	23.09	2.55	24.50	1.47	24.31	3.57
Fe_2O_3	13.50	0.31	13.37	5.81	1.22	6.22	0.24	7.00	0.21
MnO	0.56	0.03	0.40	0.62	0.20	0.43	0.05	0.61	0.28
MgO	1.21	0.13	0.57	6.83	1.96	6.06	0.94	6.32	2.53
CoO	0.03	0.02	0.02	0.04	0.03	0.03	0.02	0.01	0.01
NiO	0.08	0.03	0.00	0.09	0.06	0.12	0.03	0.14	0.03
ZnO	0.20	0.03	0.87	0.08	0.05	0.08	0.02	0.09	0.06
Total	99.39		96.39	97.72		97.45		97.66	
On the basis of four oxygen:									
Cr	1.034	0.011	0.868	1.182	0.119	1.106	0.006	1.159	0.007
Ti	0.031	0.002	0.013	0.011	0.005	0.009	0.001	0.032	0.001
V	0.008	0.001	0.006	0.006	0.001	0.005	0.001	0.008	0.000
Al	0.529	0.019	0.735	0.635	0.085	0.708	0.011	0.580	0.008
Fe^{3+}	0.357	0.009	0.358	0.147	0.029	0.158	0.006	0.180	0.008
Fe^{2+}	0.948	0.007	0.952	0.651	0.082	0.690	0.045	0.694	0.113
Mn	0.017	0.001	0.012	0.018	0.006	0.012	0.001	0.018	0.008
Mg	0.063	0.007	0.030	0.341	0.091	0.304	0.045	0.319	0.121
Co	0.001	0.001	0.001	0.001	0.001	0.001	0.001	0.000	0.000
Ni	0.002	0.001	0.000	0.002	0.002	0.003	0.001	0.004	0.001
Zn	0.005	0.001	0.023	0.002	0.001	0.002	0.000	0.002	0.001
$Cr/(Cr^{3+}+Al^{3+}+Fe^{3+})$	0.538	0.006	0.443	0.602	0.058	0.561	0.003	0.604	0.004
$Fe^{3+}/(Cr^{3+}+Al^{3+}+Fe^{3+})$	0.186	0.005	0.183	0.075	0.015	0.080	0.003	0.094	0.004
$Al/(Cr^{3+}+Al^{3+}+Fe^{3+})$	0.276	0.010	0.375	0.324	0.044	0.359	0.005	0.303	0.004
$Fe^{3+}/(Fe^{2+}+Fe^{3+})$	0.274	0.004	0.274	0.186	0.045	0.186	0.015	0.208	0.026
$Mg/(Mg^{2+}+Fe^{2+})$	0.063	0.007	0.031	0.343	0.088	0.306	0.045	0.314	0.116
$Fe^{2+}/(Mg^{2+}+Fe^{2+})$	0.937	0.007	0.969	0.657	0.088	0.694	0.045	0.686	0.116
$Cr/(Cr^{3+}+Al^{3+})$	0.661	0.010	0.542	0.650	0.052	0.610	0.005	0.666	0.004

Abbreviations: Av., average; BRS, Bird River Sill; Core, position of grain; MI, Mayville intrusion; SD, standard deviation

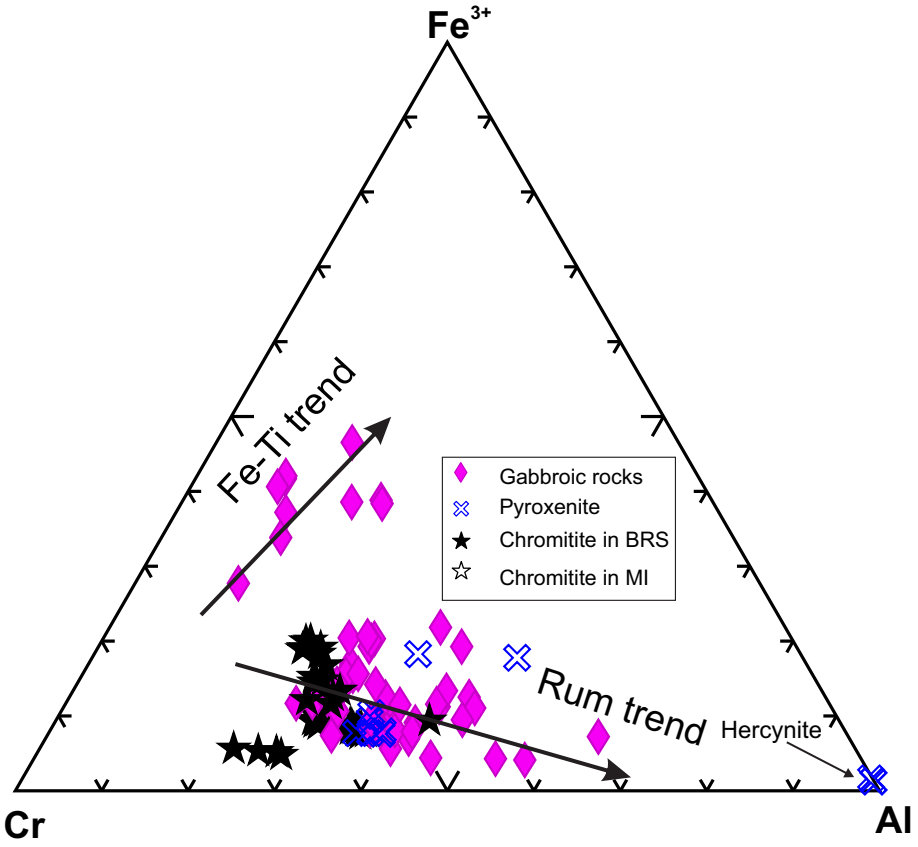

Figure GS-3-6: *Ternary plot of Cr^{3+}-Al^{3+}-Fe^{3+} in chromite from the Mayville intrusion (MI) and the Bird River sill (BRS) in the Bird River greenstone belt, southeastern Manitoba. Data are from this study, Gait (1964), and Hiebert (2003). Arrows show the Fe-Ti trend and Rum trend, as defined by Barnes and Roeder (2001). The data for chromite in gabbroic rocks and pyroxenite are from the MI.*

of enriched Fe^{3+}; the other group, together with the data from the BRS, displays a Rum trend, indicating the similarity between the two intrusions in terms of chromite chemistry, although the data from the BRS lack the Fe-Ti trend. This suggests that chromite crystallized from magmas of tholeiitic affinity that may have differentiated with fractional crystallization in a continental crust setting (cf. Barnes and Roeder, 2001). It is interpreted that these combined trends are the result of reaction between cumulus chromite crystals and evolving interstitial silicate melt, consistent with the observations of Barnes and Roeder (2001). These authors pointed out that the Rum trend is commonly restricted to layered mafic intrusions and is attributed to reaction between cumulus chromite, trapped intercumulus liquid, plagioclase and olivine.

It is noted that some of the chromite in chromitite from the BRS displays relatively low Fe^{3+} contents (Figure GS-3-6). Because the ratio of chromite to the trapped silicate liquid is so high in chromitite, the effect of the reaction between chromite and interstitial liquid on the composition of chromite may be less pronounced. Thus, chromitite is more likely to reflect the primary composition of liquidus chromite.

On the plot of Cr# versus Fe# (Figure GS-3-7), chromite from the MI appears to resemble that in Archean anorthosite complexes of Rollinson et al. (2010), showing a continuous trend, but is distinctly different from that in chromitite of the BRS. The MI chromite displays variable Cr# but relatively narrow and higher Fe#. The BRS chromite, however, has relatively constant Cr# but variable and relatively lower Fe#, which may be ascribed to the late-stage metamorphic effect proposed by Scoates et al. (1986). However, it is noted that, at a fixed Cr#, the MI chromite has a higher Fe# and lower Mg# than chromite from the BRS that had formed from relatively primitive magma(s) (i.e., higher Mg#), consistent with their geochemical signatures based on bulk-rock molar MgO/(FeO+MgO) ratios (Yang et al., 2011, 2012). This suggests that the parental magmas of both the MI and the BRS are dominantly tholeiitic in affinity but evolved via different paths: the MI is more evolved than the BRS.

In this study, hercynite ($Fe^{2+}Al_2O_4$) was not observed from the MI, although it was reported to be present as disseminations in a pyroxenite sample by Hiebert (2003). Hercynite displays the lowest Cr# and relatively lower Fe#. This mineral belongs to a distinct population in mineral

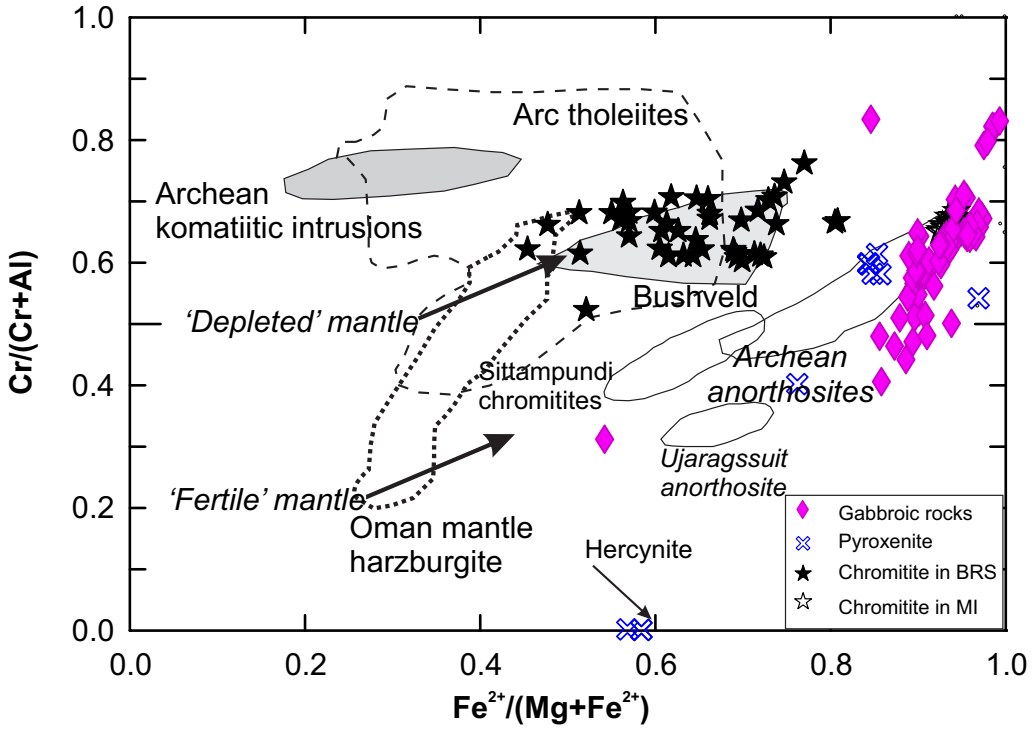

Figure GS-3-7: *Plot of Fe# versus Cr# of chromite from the Mayville intrusion and Bird River sill. Data sources and symbols as in Figure GS-3-6. Hercynite has the lowest Cr# (= 0). The fields of chromite in arc tholeiite (Barnes and Roeder, 2001), the Oman ophiolite from the 'fertile' mantle harzburgite (dotted outline; Le Mée et al., 2004), and Archean komatiitic intrusions, Bushveld complex, Archean anorthosites, Ujaragssuit anorthosite and Sittampundi chromitite (Rollinson et al., 2010) are shown. The heavy arrows show the evolution of melts from aluminous (fertile) mantle in the Archean and from less aluminous (depleted) mantle in recent arcs (after Rollinson et al., 2010).*

chemistry, as shown in Figures GS-3-6 and -7. The hercynite grains occur as disseminations in a matrix of amphibole and chlorite (Hiebert, 2003), suggesting that it may not be primary and perhaps formed during later alteration or metamorphism (e.g., Deer et al., 1962, 1992). Evidence of magmatic hercynite is rare (Kamenetsky et al., 2001). Thus, the possible petrogenetic implications are not discussed further here.

A diagram (not shown) of Fe# versus $Fe^{3+}/(Fe^{3+}+Cr+Al)$ indicates that the values for chromite from the MI are very low (<20 in most cases) and comparable to those from the BRS, and seem to increase with fractionation. This suggests that the parental magmas from which chromite crystallized might be relatively reduced, favouring the formation of sulphide minerals (Roeder, 1994). The Fe-numbers, however, are generally higher but less variable than those from the BRS, consistent with the conclusion that the MI is more evolved than the BRS (Yang et al., 2011, 2012). A plot (not shown) of Mg# $(Mg/Mg+Fe^{2+})$ against $Fe^{3+}/(Fe^{3+}+Cr+Al)$ indicates that the MI chromite has much lower Mg# (<20), whereas chromite in the BRS has higher and more variable Mg# (20–50). Again, chromite from chromitite in the BRS is broadly similar to that in chromitite from continental mafic intrusions, as compiled by Barnes and Roeder (2001), with relatively low $Fe^{3+}/(Fe^{3+}+Cr+Al)$ ratios and a range in Fe#.

Titania (wt. %) contents (not shown; see also Figure GS-3-6) increase with increasing atomic $Fe^{3+}/(Fe^{3+}+Cr+Al)$ ratios and Fe# in chromites from the MI and the BRS, a typical Fe-Ti trend commonly seen in continental mafic intrusions elsewhere, as indicated in Barnes and Roeder (2001). Chemically, chromites from these two intrusions are indistinguishable in terms of their $Fe^{3+}/(Fe^{3+}+Cr+Al)$ ratios, but the MI chromite has higher Fe#, as described above. In addition, it is noteworthy that most of the chromite has relatively low TiO_2 (<1.5 wt. %; Table GS-3-1). These values are higher than for podiform chromite (<0.3 wt. %) associated with ophiolite (e.g., Duke, 1983), but they are consistent with those crystallized from tholeiitic magmas (Kamenetsky et al., 2001) elsewhere and with the conclusions based on lithogeochemical characteristics of the MI (Peck et al., 2000, 2002; Yang et al., 2011, 2012).

It is known that trivalent (Al, Cr) and tetravalent (Ti) cations in magmatic spinel group minerals are reluctant to exchange with those in olivine during post-entrapment re-equilibration because these cations have low diffusivity in olivine compared to Mg^{2+} and Fe^{2+}. Thus, Al_2O_3 and

TiO_2 contents of spinel minerals are largely controlled by magma composition, as suggested by Kamenetsky et al. (2001), a characteristic that can be used to discriminate geodynamic settings in which the magmas formed. For example, low-Al–low-Ti spinel is related to island-arc magmas, whereas low-Al–high-Ti spinel is associated with rifting magmas in large igneous provinces. Chromites in both the MI and BRS contain relatively low Al_2O_3 and TiO_2 (Table GS-3-1), and most plot in the fields of island arc and MORB (Figure GS-3-8) with transitional features. The core compositions of chromite define a narrow range that largely straddles the boundary of island-arc magmas (ARC) and MORB, which may be compatible with a back-arc setting. According to the study of Kamenetsky et al. (2001), spinel minerals from modern back-arc environments also exhibit transitional compositions, spanning those for island arc and MORB. They suggested that back-arc magmas form in complex settings that may involve diverse melting conditions and subduction-related magma components. However, a more complicated situation is evident for the MI chromite dataset, which may be attributed to the effect of metamorphism and/or alteration. For example, Barnes (2000) and Rollinson et al. (2002) noticed that metamorphism of mid-amphibolite– to granulite-facies conditions may modify chromite chemistry, leading to enrichment in Ti^{4+}, Fe^{3+}/Fe^{2+} and Al^{3+}.

It is noteworthy that Al/Mg ratios increase with decreasing Mg# in chromite from the MI and the BRS (Figure GS-3-9). This diagram shows that the MI chromite has higher Al/Mg ratios but lower Mg# than the BRS chromite, suggesting that the MI is more evolved compared to the BRS. Again, this is consistent with the prior lithogeochemical studies mentioned above, although the ultramafic unit (pyroxenite) in the MI displays a trend similar to the latter. These chemical characteristics of chromite may reflect a petrogenetic linkage between these two intrusions. Given that their ages overlap within uncertainty (i.e., MI at 2742.8 ±0.8 Ma [Houlé et al., 2013]; BRS at 2743.0 ±0.5 Ma [Scoates and Scoates, 2013]), they were likely produced either from partial melting of a heterogeneous mantle source or via fractional crystallization of similar parental magma derived from a subcontinental lithospheric mantle. In the former case, the MI requires a more fertile mantle source, where the BRS requires a depleted mantle source. In the latter scenario, the MI may have been sourced from a more fractionated parental magma compared to that of the BRS. Analyses showing 'abnormal' compositions may be attributed to the effects of metamorphism or alteration.

Hiebert (2003) concluded that the MI and BRS were probably comagmatic, in accord with the conclusions of Macek (1985). However, the compositional differences

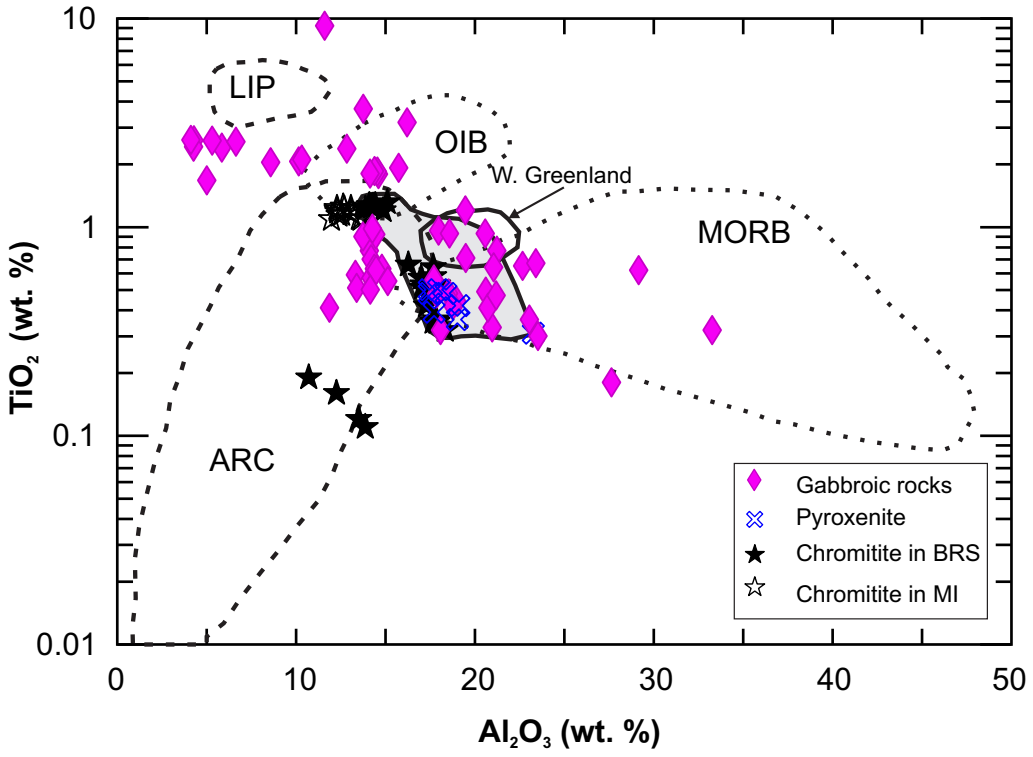

Figure GS-3-8: *Plot of TiO_2 versus Al_2O_3 contents (wt. %) in chromites from the Mayville intrusion and Bird River sill. The shaded area denotes core compositions. The discrimination fields of chromian spinel inclusions trapped in primitive olivine (Fo >84) from mid-ocean-ridge basalt (MORB), oceanic-island basalt (OIB), large igneous provinces (LIP), island-arc magmas (ARC) and west Greenland are from Kamenetsky et al. (2001). Data sources and symbols as Figure GS-3-6.*

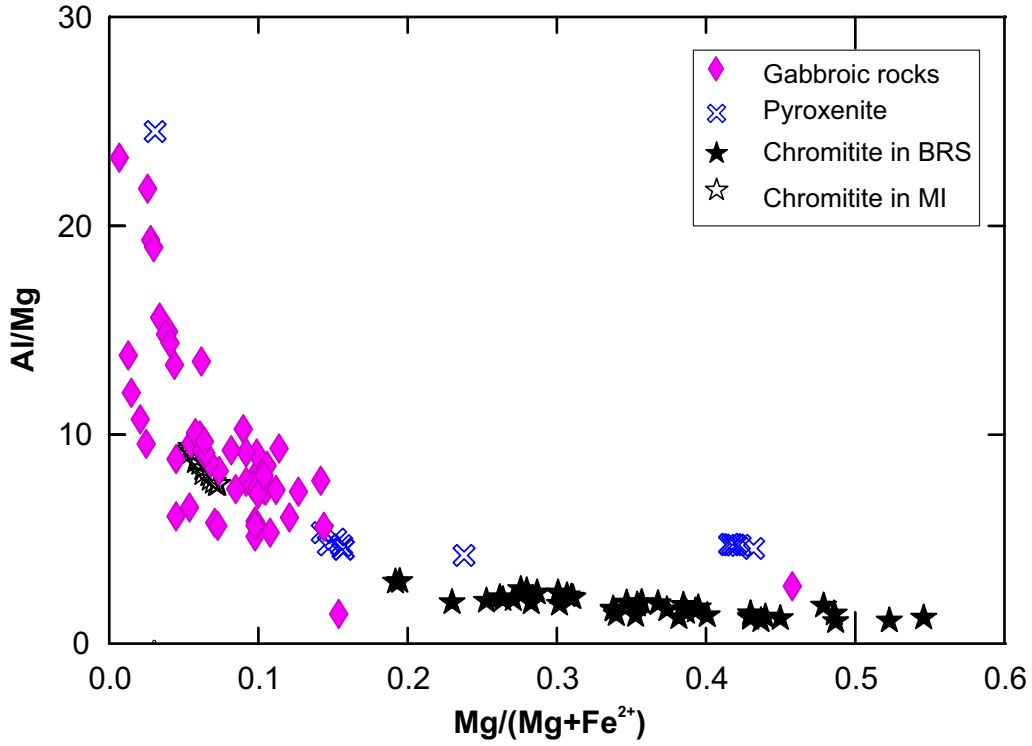

Figure GS-3-9: *Plot of Al/Mg versus Mg# ($Mg^{2+}/[Mg^{2+}+Fe^{2+}]$) in chromite from the Mayville intrusion (MI) and Bird River sill (BRS). Data sources and symbols as Figure GS-3-6.*

between the two chromite populations suggest minor differences in magmatic processes.

Minor oxides V_2O_5, NiO, CoO, ZnO and MnO in chromite were also analyzed in this study, but no anomalous values were noted (Table GS-3-1), although the MI chromite exhibits relatively lower NiO contents than the BRS. This relative depletion of Ni in the MI chromite suggests that it is prospective for magmatic Ni mineralization (e.g., Barnes and Tang, 1999).

Discussion

Three mechanisms have commonly been cited to explain crystallization of chromite from a mafic–ultramafic magmatic system to form chromitite seams or layers: fractional crystallization, contamination by sialic material and magma mixing (Irvine, 1975, 1977; Marques et al., 2003). Elevation of oxygen fugacity (fO_2) may also trigger chromite precipitation (Ulmer, 1969). Talkington et al. (1983) suggested that increasing fO_2 could occur by wallrock assimilation or new magma injection. Liquid immiscibility was also proposed for the origin of chromitite seams in layered mafic–ultramafic intrusions (McDonald, 1965).

In the Chromitiferous zone of the BRS (Figures GS-3-4, -5a), chromite appears to have crystallized after olivine. Fractional crystallization of olivine drove the melt composition toward the olivine-chromite cotectic line, where chromite coprecipitated with olivine until the appearance of orthopyroxene. This model is consistent with field investigations and petrography (Scoates et al., 1986, 1989), which document olivine cumulates at the base, olivine-chromite cumulates in the middle, and chromitite (chromite cumulates) and pyroxene cumulates at the top of each igneous unit. Alternatively, fresh primitive magma fluxing into the magma chamber and mixing with evolving magmas could result in chromite crystallization and formation of chromitite layers (e.g., Irvine, 1977; Scoates et al., 1989). Field relationships are consistent with the scenario of multiple injections of magma having taken place within the BRS (Mealin, 2008), which is a composite intrusion similar to the MI in this regard.

Crystallization of calcic plagioclase (Yang, unpublished data, 2013) resulted in alumina depletion and chrome build-up in the magmatic systems that contain up to 5% water, depending upon pressures suggested in the experimental study of Takagi et al. (2005). Thus, at the chromitite stage, chromite crystallized from mafic–ultramafic magma(s) relatively poor in Al_2O_3 but rich in mafic components. Crystallization of chromite led to the magma gradually becoming enriched in Al but depleted in Mg, reflecting a decrease of Mg# and an increase of Al/Mg ratio in the MI chromite (Figure GS-3-9).

The chemistry of chromite, lithogeochemistry and experimental constraints require a hydrous, high-Al tholeiitic magma(s) parental to the MI. The magma reached liquidus with cooling, and started to crystallize

calcic plagioclase, then plagioclase+chromite, plagioclase+chromite+amphibole (after pyroxene) and chromite+amphibole (after pyroxene). Recrystallization of plagioclase may have occurred during later deformation and greenschist to amphibolite metamorphism to produce a granular texture within former megacrysts, similar to what is observed in the Fiskenæsset anorthositic complex of west Greenland (Windley and Garde, 2009; Rollinson et al., 2010).

Chromite may form distinct bands due to crystal sorting and accumulation, or igneous sedimentation processes, in a layered mafic–ultramafic intrusion; if sufficiently concentrated, a chromite deposit could form, as evidenced by the BRS and the Euclid Lake intrusion (Watson, 1985).

Further work is required for the MI and BRS chromites, as they may be used to estimate intracrystalline closure temperatures (T_c; Princivalle et al., 1999; Lenaz et al., 2004, 2011; Lucchesi et al., 2010) and fO_2 (Ballhaus et al., 1991). Such work may provide more information on the cooling rate of these intrusions and factors controlling the formation of sulphide minerals and chromitite.

Economic considerations

The Mayville intrusion (MI) is a composite mafic–ultramafic intrusion that was emplaced broadly coeval with the Bird River sill (BRS). These intrusions are attributed to the Neoarchean 'Bird River magmatic event' (Houlé et al., 2013), which is associated with several significant deposits of magmatic Ni-Cu-PGE and Cr in Manitoba and along strike to the east in Ontario (i.e., the 'Ring of Fire'). Mineral resources in the MI were recently updated by Mustang Minerals Corp. to include 26.6 Mt grading 0.18% Ni, 0.44% Cu and 0.24 g/t combined Pt+Pd+Au in the indicated category, and 5.2 Mt at similar grade in the inferred category (Mustang Minerals Corp., 2014). The Bird River chromite deposit includes an historical resource of 60 Mt grading 3.88% Cr_2O_3 (Watson, 1985), which represented the major repository of chromite resource in Canada prior to the discovery of the McFaulds Lake deposits (i.e., the Ring of Fire) in northern Ontario.

In this study, chromite chemistry is used as a 'petrogenetic indicator' to investigate the nature of mafic–ultramafic magmas parental to the MI and the BRS, their possible magmatic evolution and the potential tectonic setting of the Bird River greenstone belt, and to provide insights into several key aspects relevant to exploration for magmatic Ni-Cu-PGE-(Cr) deposits, such as affinity (nature) and fertility of magmas, processes of magmatic evolution and regional tectonic setting. These new data can help to determine where and why magmatic Ni-C-PGE-Cr mineralization occurs, but they must be used in conjunction with detailed geological mapping and lithogeochemistry. Chemical compositions of MI chromite indicate that the parental magma(s) is/are tholeiitic and may have been derived from subcontinental lithospheric mantle enriched by slab melts with tonalite, trondhjemite and granodiorite affinity (the slab melt may be represented by the quartz diorite–tonalite dikes cutting the heterolithic breccia zone, as shown in Figure GS-3-2) due to plate subduction. This scenario was also proposed by Rollinson et al. (2010) for the genesis of the Archean anorthosite suite in western Greenland. The MI is considered favourable for magmatic Ni-Cu-PGE-(Cr) mineralization, given that it was emplaced into suitable supracrustal rocks, such as the sulphide-bearing metasedimentary rocks to the north, that might provide the external sulphur required for sulphur saturation and precipitation of sulphide.

Acknowledgments

The authors thank L. Lafreniere, S. Kushner and D. Drayson for providing enthusiastic field assistance, as well as E. Anderson and N. Brandson for thorough logistical support. We thank R. Sidhu at the University of Manitoba for assistance in electron probe microanalysis; C. Galeschuk with Mustang Minerals Corp. for allowing us to access to the company's mineral properties and data; and M. Houlé and V. Bécu with the Geological Survey of Canada for field discussion and collaboration. Constructive reviews by S. Gagné and S. Anderson, and technical editing by B. Davie are gratefully acknowledged.

References

Arif, M. and Jan, M.Q. 2006: Petrotectonic significance of the chemistry of chromite in the ultramafic-mafic complexes of Pakistan; Journal of Asian Earth Sciences, v. 27, p. 628–646.

Bailes, A.H., Percival, J.A., Corkery, M.T., McNicoll, V.J., Tomlinson, K.Y., Sasseville, C., Rogers, N., Whalen, J.B. and Stone, D. 2003: Geology and tectonostratigraphic assemblages, West Uchi map area, Manitoba and Ontario; Manitoba Geological Survey, Open File OF2003-1, Geological Survey of Canada, Open File 1522, Ontario Geological Survey, Preliminary Map P.3461, 1:250 000 scale.

Ballhaus, C., Berry, R.F. and Green, D.H. 1991: High pressure experimental calibration of the olivine-orthopyroxene-spinel oxygen geobarometer: implications for the oxidation state of the upper mantle; Contributions to Mineralogy and Petrology, v. 107, p. 27–40.

Barnes, S.J. 1998: Chromite in komatiite, I — magmatic controls on crystallization and composition; Journal of Petrology, v. 39, p. 1689–1720.

Barnes, S.J. 2000: Chromite in komatiite, II — modification during greenschist to mid-amphibolite facies metamorphism; Journal of Petrology, v. 41, p. 389–409.

Barnes, S.J. and Kunilov, V.Y. 2000: Spinels and Mg ilmenites from the Noril'sk 1 and Talnakh intrusions and other mafic rocks of the Siberian flood basalt province; Economic Geology, v. 95, p. 1701–1717.

Barnes, S.J. and Roeder, P.L. 2001: The range of spinel compositions in terrestrial mafic and ultramafic rocks; Journal of Petrology, v. 42, p. 2279–2302.

Barnes, S.J. and Tang, Z.-L. 1999: Chrome spinels from the Jinchuan Ni-Cu sulfide deposit, Gansu Province, People's Republic of China; Economic Geology, v. 94, p. 343–356.

Bateman, J.D. 1943: Bird River chromite deposits, Manitoba; Canadian Institute of Mining and Metallurgy Transactions, v. 46, p. 154–183.

Bateman, J.D. 1945: Composition of the Bird River chromite, Manitoba; American Mineralogist, v. 30, p. 596–600.

Brownell, G.M. 1942: Chromite in Manitoba; Precambrian, v. 15, no. 12, p. 3–5.

Deer, W.A., Howie, R.A. and Zussman, J. 1962: Rock forming minerals: volume 5 — non-silicates; Longmans, London, United Kingdom, 371 p.

Deer, W.A., Howie, R.A. and Zussman, J. 1992: An introduction to the rock-forming minerals, second edition; Longmans, Essex, United Kingdom, 696 p.

Duguet, M., Lin, S., Davis, D.W., Corkery, M.T. and McDonald, J. 2009: Long-lived transpression in the Archean Bird River greenstone belt, western Superior province, southeastern Manitoba; Precambrian Research, v. 174, no. 3–4, p. 381–407.

Duke, J.M. 1983: Magmatic segregation deposits of chromite; Geoscience Canada, v. 10, p. 15–24.

Gait, R.I. 1964: The mineralogy of the chrome spinels of the Bird River Sill, Manitoba; M.Sc. thesis, University of Manitoba, Winnipeg, Manitoba, 64 p.

Gilbert, H.P., Davis, D.W., Duguet, M., Kremer, P.D., Mealin, C.A. and MacDonald, J. 2008: Geology of the Bird River Belt, southeastern Manitoba (parts of NTS 52L5, 6); Manitoba Science, Technology, Energy and Mines, Manitoba Geological Survey, Geoscientific Map MAP2008-1, scale 1:50 000 (plus notes and appendix).

Hiebert, R. 2003: Composition and genesis of chromite in the Mayville intrusion: southeastern Manitoba; B.Sc. thesis, University of Manitoba, Winnipeg, Manitoba, 96 p.

Houlé, M.G., McNicoll, V.J., Bécu, V., Yang, X.M. and Gilbert, H.P. 2013: New age for the Mayville intrusion: implication for a large mafic–ultramafic event in the Bird River greenstone belt, southeastern Manitoba (abstract); Geological Association of Canada–Mineralogical Association of Canada, Joint Annual Meeting, Winnipeg, Manitoba, May 22–24, 2013, Program with Abstracts, p. 115.

Irvine, T.N. 1965: Chromian spinel as a petrogenetic indicator, part I: theory; Canadian Journal of Earth Sciences, v. 2, p. 648–672.

Irvine, T.N. 1967: Chromian spinel as a petrogenetic indicator, part II: petrologic application; Canadian Journal of Earth Sciences, v. 4, p. 71–103.

Irvine, T.N. 1975: Crystallization sequences in the Muskox intrusion and other layered intrusions, II: origin of chromitite layers and similar deposits of other magmatic ores; Geochimica et Cosmochimica Acta, v. 39, p. 991–1020.

Irvine, T.N. 1977: Origin of chromitite layers in the Muskox intrusion and other stratiform intrusions: a new interpretation; Geology, v. 5, p. 273–277.

Kamenetsky, V.S., Crawford, A.J. and Meffre, S. 2001: Factors controlling chemistry of magmatic spinel: an empirical study of associated olivine, Cr-spinel and melt inclusions from primitive rocks; Journal of Petrology, v. 42, p. 655–671.

Krause, J., Brügmann, G.E. and Pushkarev, E.V. 2011: Chemical composition of spinel from Uralian-Alaskan–type mafic-ultramafic complexes and its petrogenetic significance; Contributions to Mineralogy and Petrology, v. 161, p. 255–273.

Le Mée, L., Girardeau, J. and Monnier, C. 2004: Mantle segmentation along the Oman ophiolite fossil midocean ridge; Nature, v. 432, p. 167–172.

Lemkow, D.R., Sanborn-Barrie, M., Bailes, A.H., Percival, J.A., Rogers, N., Skulski, T., Anderson, S.D., Tomlinson, K.Y., McNicoll, V., Parker, J.R., Whalen, J.B., Hollings, P. and Young, M. 2006: GIS compilation of geology and tectonostratigraphic assemblages, western Uchi Subprovince, western Superior Province, Ontario and Manitoba; Manitoba Industry, Economic Development and Mines, Manitoba Geological Survey, Open File Report OF2006-30, 1 CD-ROM, scale 1:250 000.

Lenaz, D., Andreozzi, G.B., Mitra, S., Bidyananda, M. and Princivalle, F. 2004: Crystal chemical and ^{57}Fe Mössbauer study of chromite from the Nuggihalli schist belt (India); Mineralogy and Petrology, v. 80, p. 45–57.

Lenaz, D., O'Driscoll, B. and Princivalle F. 2011: Petrogenesis of the anorthosite-chromitite association: crystal-chemical and petrological insights from the Rum Layered Suite, NW Scotland; Contributions to Mineralogy and Petrology, v. 162, p. 1201–1213.

Lucchesi, S., Bosi, F. and Pozzuoli, A. 2010: Geothermometric study of Mg-rich spinels from the Somma-Vesuvius volcanic complex (Naples, Italy); American Mineralogist, v. 95, p. 617–621.

Macek, J.J. 1985: Cat Creek project (parts of 52L/1, 8); *in* Report of Activities 1985, Manitoba Energy and Mines, Mineral Resources Division, p. 122–129.

Marques, J.C., Ferreira Filho, C.F., Carlson, R.W. and Pimentel, M.M. 2003: Re-Os and Sm-Nd isotope and trace element constraints on the origin of the chromite deposits of the Ipueira-Medrado sill, Bahia, Brazil; Journal of Petrology, v. 44, p. 659–678.

McDonald, J.A. 1965: Liquid immiscibility as one factor in chromite seam formation in the Bushveld Igneous Complex; Economic Geology, v. 60, p. 1674–1685.

Mealin, C.A. 2008: Geology, geochemistry and Cr-Ni-Cu-PGE mineralization of the Bird River sill: evidence for a multiple intrusion model; MSc thesis, University of Waterloo, Waterloo, Ontario, 155 p.

Mustang Minerals Corp. 2014: Mustang files NI 43-101 PEA on nickel-copper-PGM project in southeastern Manitoba; Mustang Minerals Corp., press release, May 26, 2014, URL <http://www.mustangminerals.com/admin/news/86.pdf> [August 2014].

Nickel, E.H. 1992: Solid solutions in mineral nomenclature; Mineralogical Magazine, v. 56, p. 127–130.

Ohnenstetter, D., Watkinson, D.H., Jones, P.C. and Talkington, W. 1986: Cryptic compositional variation in laurite and enclosing chromite from the Bird River Sill, Manitoba; Economic Geology, v. 81, no. 5, p. 1159–1168.

Peck, D.C. and Keays, R.R. 1990: Geology, geochemistry, and origin of platinum-group element-chromitite occurrences in the Heazlewood River Complex, Tasmania; Economic Geology, v. 85, p. 975–793.

Peck, D.C., Scoates, R.F.J., Theyer, P., Desharnais, G., Hulbert, L.J. and Huminicki, M.A.E. 2002: Stratiform and contact-type PGE-Cu-Ni mineralization in the Fox River Sill and the Bird River Belt, Manitoba; *in* The Geology, Geochemistry, Mineralogy and Mineral Beneficiation of Platinum-Group Elements, L.J. Cabri (ed.), Canadian Institute of Mining and Metallurgy, Special Volume 54, p. 367–387.

Peck, D.C., Theyer, P., Bailes, A.H. and Chornoby, J. 1999: Field and lithogeochemical investigations of mafic and ultramafic rocks and associated Cu-Ni-PGE mineralization in the Bird River greenstone belt (parts of NTS 52L); *in* Report of Activities, 1999, Manitoba Industry, Trade and Mines, Geological Services, p. 106–110.

Peck, D.C., Theyer, P., Hulbert, L., Xiong, J., Fedikow, M.A.F. and Cameron, H.D.M. 2000: Preliminary exploration database for platinum-group elements in Manitoba; Manitoba Industry, Trade and Mines, Manitoba Geological Survey, Open File OF2000-5, CD-ROM.

Princivalle, F., Della Giusta, A., De Min, A. and Piccirillo, E.M. 1999: Crystal chemistry and significance of cation ordering in Mg-Al rich spinels from high-grade hornfels (Predazzo-Mononi, NE Italy); Mineralogical Magazine, v. 63, p. 257–262.

Rollinson, H.R., Appel, P.W.U. and Frei, R. 2002: A metamorphosed, Early Archean chromitite from West Greenland: implications for the genesis of Archaean anorthositic chromitites; Journal of Petrology, v. 43, p. 2143–2170.

Rollinson, H.R., Reid, C. and Windley, B. 2010: Chromitites from the Fiskenæsset anorthositic complex, West Greenland: clues to late Archaean mantle processes; *in* The Evolving Continents: Understanding Processes of Continental Growth, T.M. Kusky, M.-G. Zhai and W. Xiao, (ed.), Geological Society, London, Special Publications, v. 338, p. 197–212.

Roeder, P.L. 1994: Chromite: from the fiery rain of chondrules to the Kilauea Iki lava lake; Canadian Mineralogist, v. 32, p. 155–196.

Scoates, R.F.J. 1983: A preliminary stratigraphic examination of the ultramafic zone of the Bird River Sill, southeastern Manitoba; *in* Report of Field Activities 1983, Manitoba Department of Energy and Mines, Mineral Resources Division, p. 70–83.

Scoates, J.S. and Scoates, R.F.J. 2013: Age of the Bird River Sill, southeastern Manitoba, Canada, with implications for the secular variation of layered intrusion–hosted stratiform chromite mineralization; Economic Geology, v. 108, p. 895–907.

Scoates, R.F.J., Williamson, B.L. and Duke, J.M. 1986: Igneous layering in the Ultramafic Series, Bird River Sill; *in* Layered intrusions of southeastern Manitoba and northwestern Ontario, R.F.J. Scoates, B.L. Williamson, J.M. Duke, W. Mandziuk, W.C. Brisbin and R.H. Sutcliffe (ed.), Geological Association of Canada, Field Trip 13 Guidebook, May 12–14, 1986, p. 1–19.

Scoates, R.F.J., Williamson, B.L., Eckstrand, O.R. and Duke, J.M. 1989: Stratigraphy of the Bird River Sill and its chromitiferous zone, and preliminary geochemistry of the chromitite layers and PGE-bearing units, Chrome property, Manitoba; *in* Investigations by the Geological Survey of Canada in Manitoba and Saskatchewan during the 1984–1989 Mineral Development Agreements, A.G. Galley (ed.), Geological Survey of Canada, Open File 2133, p. 69–82.

Stevens, R.E. 1944: Compositions of some chromites of the western hemisphere; American Mineralogist, v. 29, p. 1–34.

Sobolev, N.V. and Logvinova, A.M. 2005: Significance of accessory chrome spinel in identifying serpentinite paragenesis; International Geology Review, v. 47, p. 58–64.

Stevenson, R., Machado, N., Bernier, F. and Courteau, G. 2001: Nd isotopic studies of the buried Precambrian crust in southern Manitoba; *in* 2001 Western Superior Transect Seventh Annual Workshop, R.M. Harrap and H.H. Helmstaedt (ed.), LITHOPROBE Secretariat, University of British Columbia, Vancouver, British Columbia, Report 80, p. 17–25.

Stowe, C.W. 1994: Compositions and tectonic settings of chromite deposits through time; Economic Geology, v. 89, p. 528–546.

Takagi, D., Sato, H. and Nakagawa, M. 2005: Experimental study of low alkali tholeiite at 1–5 kbar: optimal condition for the crystallisation of high-An plagioclase in hydrous arc tholeiite; Contributions to Mineralogy and Petrology, v. 149, p. 527–540.

Talkington, W., Watkinson, D.H., Whittaker, P.J. and Jones, P.C. 1983: Platinum-group mineral inclusions in chromite from the Bird River Sill, Manitoba; Mineralium Deposita, v. 18, no. 2A, p. 245–255.

Theyer, P. 1991: Petrography, chemistry and distribution of platinum and palladium in ultramafic rocks of the Bird River Sill, SE Manitoba, Canada; Mineralium Deposita, v. 26, no. 3, p. 165–174.

Theyer, P. 2003: Platinum group element investigations in the Mayville igneous complex, southeastern Manitoba (NTS 52L12); *in* Report of Activities 2003, Manitoba Industry, Trade and Mines, Manitoba Geological Survey, p. 196–199.

Trueman, D.L. 1980: Stratigraphy, structure and metamorphic petrology of the Archean greenstone belt at Bird River, Manitoba; Ph.D. thesis, University of Manitoba, Winnipeg, Manitoba, 150 p.

Ulmer, G.C. 1969: Experimental investigations of chromite spinels; Economic Geology Monograph 4, p. 114–131.

Voigt, M. and von der Handt, A. 2011: Influence of subsolidus processes on the chromium number in the spinel in ultramafic rocks; Contributions to Mineralogy and Petrology, v. 162, p. 675–689.

Watson, D.M. 1985: Chromite reserves of the Bird River Sill; Manitoba Energy and Mines, Geological Services, Open File Report OF85-8, 22 p.

Williamson, B.L. 1990: Geology of the Bird River Sill at the Chrome property, southeast Manitoba; Geological Survey of Canada, Open File 2067, 44 p.

Windley, B.F. and Garde, A.A. 2009: Arc-generated blocks with crustal sections in the North Atlantic craton of West Greenland: crustal growth in the Archean with modern analogues; Earth-Science Reviews, v. 93, p. 1–30.

Yang, X.M. 2014: Bedrock geology of the Cat Creek area, Bird River greenstone belt, southeastern Manitoba (part of NTS 52L12); Manitoba Mineral Resources, Manitoba Geological Survey, Preliminary Map PMAP2014-3, scale 1:10 000.

Yang, X.M. and Gilbert, H.P. 2014: Archean tonalite-trondhjemite-granodiorite (TTG) suite in the Bird River greenstone belt, southeastern Manitoba: lithogeochemical characteristics, geodynamic evolution, and potential for porphyry Cu-(Au) mineralization [abstract]; Geological Association of Canada–Mineralogical Association of Canada, Joint Annual Meeting, Fredericton, New Brunswick, May 21–23, 2014, Program with Abstracts, p. 294.

Yang, X.M., Gilbert, H.P., Corkery, M.T. and Houlé, M.G. 2011: The Mayville mafic–ultramafic intrusion in the Neoarchean Bird River greenstone belt, southeastern Manitoba (part of NTS 52L12): preliminary geochemical investigation and implication for PGE-Ni-Cu-(Cr) mineralization; *in* Report of Activities 2011, Manitoba Innovation, Energy and Mines, Manitoba Geological Survey, p. 127–142.

Yang, X.M., Gilbert, H.P. and Houlé, M.G. 2012: Geological investigations of the Cat Creek area in the Neoarchean Bird River greenstone belt, southeastern Manitoba (part of NTS 52L12): new insights into PGE-Ni-Cu-Cr mineralization; *in* Report of Activities 2012, Manitoba Innovation, Energy and Mines, Manitoba Geological Survey, p. 32–53.

Yang, X.M., Gilbert, H.P. and Houlé, M.G. 2013: Cat Lake–Euclid Lake area in the Neoarchean Bird River greenstone belt, southeastern Manitoba (parts of NTS 52L11, 12): preliminary results of bedrock geological mapping and their implications for geodynamic evolution and metallogeny; *in* Report of Activities 2013, Manitoba Mineral Resources, Manitoba Geological Survey, p. 70–84.

Yang, X.Z., Matsueda, H. and Ishihara, S. 1994: Mode of occurrence, chemical composition, and origin of Cr-Fe-Ti oxides of the Jinchuan Ni-Cu-PGE deposits, China; International Geology Review, v. 36, p. 311–327.